



# Fabrication of non-flaking, superhydrophobic surfaces using a one-step solution-immersion process on copper foams



Jia Xu<sup>a</sup>, Jinliang Xu<sup>a,\*</sup>, Yang Cao<sup>b</sup>, Xianbing Ji<sup>a</sup>, Yuying Yan<sup>c</sup>

<sup>a</sup> Beijing Key Laboratory of Low-grade Energy Multiphase Flow and Heat Transfer, School of Renewable Energy, North China Electric Power University, Changping District, Beinong Road, Beijing 102206, China

<sup>b</sup> Functional Nanomaterials Laboratory and Key Laboratory of Photochemical Conversion and Optoelectronic Materials, Technical Institute of Physics and Chemistry, Chinese Academy of Sciences (CAS), Beijing 100190, China

<sup>c</sup> Energy & Sustainability Research Division, Faculty of Engineering, University of Nottingham, Nottingham NG7 2RD, UK

## ARTICLE INFO

### Article history:

Received 29 May 2013

Received in revised form 8 September 2013

Accepted 8 September 2013

Available online 16 September 2013

### Keywords:

Superhydrophobic surface

Non-flaking

Copper foam

One-step solution-immersion process

Micro- and nano-scale hierarchical morphology

## ABSTRACT

Non-flaking superhydrophobic surfaces were prepared using a simple one-step solution-immersion process on commercially obtained copper foam substrates. Copper foams were immersed in a 0.05 M ethanolic stearic acid solution at room temperature for several days. This formed coverage of copper stearate with micro- and nano-scale hierarchical surface morphology. The surface of the copper foam after 4 days of immersion demonstrates superhydrophobicity with a water contact angle of 156°. A sliding angle of 4° for a 5 μL droplet indicates excellent non-sticking behavior. Compared with a flat copper plate, the superhydrophobic surfaces based on copper foams are much more robust and mechanically stable. This work provides a promising strategy for scalable fabrication of superhydrophobic surfaces on 3D porous structures.

© 2013 Elsevier B.V. All rights reserved.

## 1. Introduction

Some biological materials have special wettability. Artificial lotus-leaf-like superhydrophobic surfaces have a water contact angle (CA) greater than 150° and a sliding angle (SA) of less than 10°. Interdisciplinary fields including biology, physics, chemistry, materials science and engineering thermal physics have investigated such materials [1–4]. Ongoing efforts have been devoted to exploring the fabrication of superhydrophobic surfaces for practical applications such as oil–water separation [5], friction reduction [6], corrosion prevention [7], highly functional microfluidic devices [8–10], and drop-wise condensation [11]. As a widely used industrial material, copper is attractive for its high electrical and thermal conductivity, mechanical workability, and malleability; however, it is susceptible to corrosion. It has recently been reported that forming superhydrophobic films on copper surfaces can effectively improve their corrosion resistance [12–14]. So far, copper with superhydrophobic surfaces has been fabricated using various strategies. These techniques include electroless galvanic deposition [15], sol–gel processing [16], surface oxidation [17], electro-deposition [18], electro-plating [19], and etching [20]. Both

micro- and nano-scale hierarchical structures and low-surface-energy materials are vital to the superhydrophobicity of a surface. As such, most fabrication procedures are divided as two steps where the hierarchical roughness is created first and subsequent modifications include low-surface-energy coatings.

The one-step solution-immersion method is one of the simplest approaches to fabricate superhydrophobic surfaces on various substrates, including zinc, silicon and steel [21]. The first report of a one-step solution-immersion process to create superhydrophobic films on copper substrates was by Jiang and co-workers [22]. In their work, hierarchical roughness and low-surface-energy were obtained simultaneously by immersing a copper plate into a fatty acid solution. Direct-current electro-deposition on copper substrates using ethanol solutions of *n*-tetradecanoic acid [23] or stearic acid [24] as electrolytes and spray-coating methods using copper stearate [25] can shorten the preparation time needed for the one-step processes. However, these approaches require additional processing steps and control of other key parameters, making them more complicated than the simple solution-immersion method. Because of its relatively few experimental parameters and long preparation time, the one-step solution-immersion method is particularly appropriate for exploring how the surface morphology evolves with preparation time, and allows us to capture details that might perhaps not be observed if we used faster approaches.

\* Corresponding author. Tel.: +86 10 61772268; fax: +86 10 61772268.  
E-mail addresses: [xjl@ncepu.edu.cn](mailto:xjl@ncepu.edu.cn), [jia.xu116@gmail.com](mailto:jia.xu116@gmail.com) (J. Xu).

The as-prepared superhydrophobic films are composed of copper fatty acid carboxylates. As there is a phase interface between the substrate and the superhydrophobic film, heat or external mechanical forces may affect the robustness of the films. However, stability is a key factor in developing the practical use of superhydrophobic films. Further investigation into increasing film stability should be carried out. Discontinuous surfaces can allow stress to be released at the edges and prevent heterogeneous layers from detaching [26]. Using copper with a discontinuous surface (rather than a flat one) as the substrate in the one-step solution-immersion approach may allow formation of a superhydrophobic surface with more robust adhesion to the substrate. 3D porous copper films have a discontinuous copper surface and have been prepared using a hydrogen bubble dynamic template. Superhydrophobicity after treatment with *n*-hendecane thiol has been demonstrated [27]. Open cell copper metal foams are a commercial obtained 3D porous material widely utilized in flat heat pipes and thermal spreaders because of its high surface area and capillary pumping capacity [28]. And their wetting properties, such as wettability transition, have been studied intensively [29]. If they can be applied to the fabrication of superhydrophobic surfaces, the preparation of 3D porous films can be simplified.

In this study, we selected copper metal foam as the substrate for fabricating a superhydrophobic surface. The superhydrophobic surface is prepared by immersing copper foam into a ethanol solution of stearate acid, with chemical reactions occurring between the copper and stearate acid. In contrast to the superhydrophobic surfaces more commonly formed on flat copper plates, the superhydrophobic surfaces prepared on the copper foam show a large surface area and non-flaking copper stearate coverage of the micro- and nano-scale hierarchical morphology. An abrasion test shows that the superhydrophobicity of the copper foam surface is more stable than that of the flat copper plate.

## 2. Experimental

Copper foams of 99.9% purity, 0.88 porosity, with 90 pores per inch (PPI) and a thickness of 2.5 mm were commercially obtained. Experimental results testing the copper plates (99.9% purity, 0.8 mm thickness) were compared with that of the copper foam samples. In this study, the copper foams and plates were cut into square pieces with side lengths of 2.0 cm. In the cleaning procedure, the copper foams and plates were sequentially washed with acetone, ethanol, 2 M HCl, and deionized (DI) water in an ultrasonic bath followed by drying with nitrogen gas. The cleaned substrates were then immersed in an ethanolic stearic acid solution (0.05 M) at room temperature. They were finally rinsed thoroughly with ethanol and DI water, and then dried in air.

Abrasion tests were carried out as described in Refs. [20,30,31]. A copper substrate with a superhydrophobic surface was subjected to a pressure of 5 kPa. As cotton fibers can be hooked by the copper foam, common A4 paper was used as a sliding base rather than the cotton fabric used in the reference.

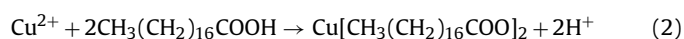
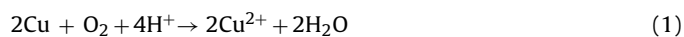
Field-emission scanning electron microscope (FE-SEM) images were obtained at 10 kV using LEO 1530 FE-SEM. Fourier transform IR (FTIR) data were collected on a Varian 3100 instrument using the KBr method as the transmission mode. Some powder was scraped from the resultant surfaces, and mixed with KBr to make a palette. X-ray photoelectron spectroscopy (XPS) data were obtained on PHI-5300 ESCA with the C 1s reference at 284.8 eV. Water CAs and SAs were measured by a contact angle meter at room temperature (OCA15EC, DataPhysics Instruments GmbH, Germany). At least five different sections were tested for each sample. 5  $\mu$ L was used for all individual water droplets.

## 3. Results and discussion

As shown in Fig. 1(a), the bare copper foam has a 3D porous frame with pore size of less than 400  $\mu$ m. Its surface is relatively flat, without any deposits, as can be seen from the magnified FE-SEM image of the copper skeleton (inset in Fig. 1(a)). Fig. 1(b)–(g) respectively illustrate the surface morphologies of the copper foams prepared with immersion times of 4 h, 2 days, and 4 days. The panoramic surface morphology of a 4 h immersion time sample (Fig. 1(b)) is similar to that of the bare copper foam, in that the outline of the copper foam skeleton is still smooth. However, there is also indication of many self-assembled clusters of a copper compound. This compound was later confirmed to be copper stearate, and the coverage of the clusters on the substrate is not dense (Fig. 1(c)). The inset in Fig. 1(c) gives a high-magnification image of the self-assembled cluster, showing that the folded copper stearate nanosheets are entangled with each other. When the immersion time increased to 2 days, the outline of the skeleton became rougher, as shown in Fig. 1(d) and the pore size was reduced as the result of copper stearate cluster growth. The magnified FE-SEM images in Fig. 1(e) reveal that dense clusters are formed and completely cover the substrate. For immersion times of 4 days, the skeleton of the 3D porous structure became thicker and rougher, and the pore size decreased significantly to  $\sim$ 100  $\mu$ m (Fig. 1(f)). The surface is now heavily covered with the self-assembled clusters. Flowerlike self-assembled clusters are also observed to have formed on top of previously laid-down cluster layers, as shown in Fig. 1(g). These cluster-flowers with the scale of about 10–20  $\mu$ m are composed of nanosheets, separated by a few microns (within one cluster-flower); adjacent cluster-flowers are also separated by several-micron gaps. This indicates that hierarchical micro-/nano-structures can be formed on the surface of the copper foams. Fig. 1(h) shows a photograph of the complete blue coating that forms on the copper foam after immersion for 4 days.

The one-step solution-immersion process was also carried out on flat copper plates. To make a straightforward comparison, the surface morphologies of copper plates, prepared using the same immersion times as those used to treat the copper foams shown in Fig. 1, were characterized by FE-SEM, and the images are presented in Fig. 2. Fig. 2(a) shows that after an immersion time of 4 h, the copper plate is sparsely covered by some deposits. These deposits are separated, flower-like clusters, about 15  $\mu$ m across (Fig. 2(b)). When the immersion time increased to 2 days, more and more deposits were formed, but some of them flaked off, as shown in Fig. 2(c) and (d). Even when the immersion time was increased to 4 days, a continuous coating was not formed (Fig. 2(e) and (f)). This is also apparent from the photograph of the copper plate prepared using an immersion time of 4 days (Fig. 2(g)). In contrast to the complete blue coating on the copper foam shown in Fig. 1(h), the coverage of the copper plate substrate is incomplete, and white. The different colors of the coatings on the copper foam and copper plate can be attributed to their different thicknesses.

Copper carboxylate has been reported to be produced by utilizing the chemical reactions between copper and fatty acid in the ethanol solution [22,24].  $\text{Cu}^{2+}$  ions are released from the substrates through the oxidation of copper and immediately react with stearic acid molecules to form copper stearate. The reaction can be expressed as follows:



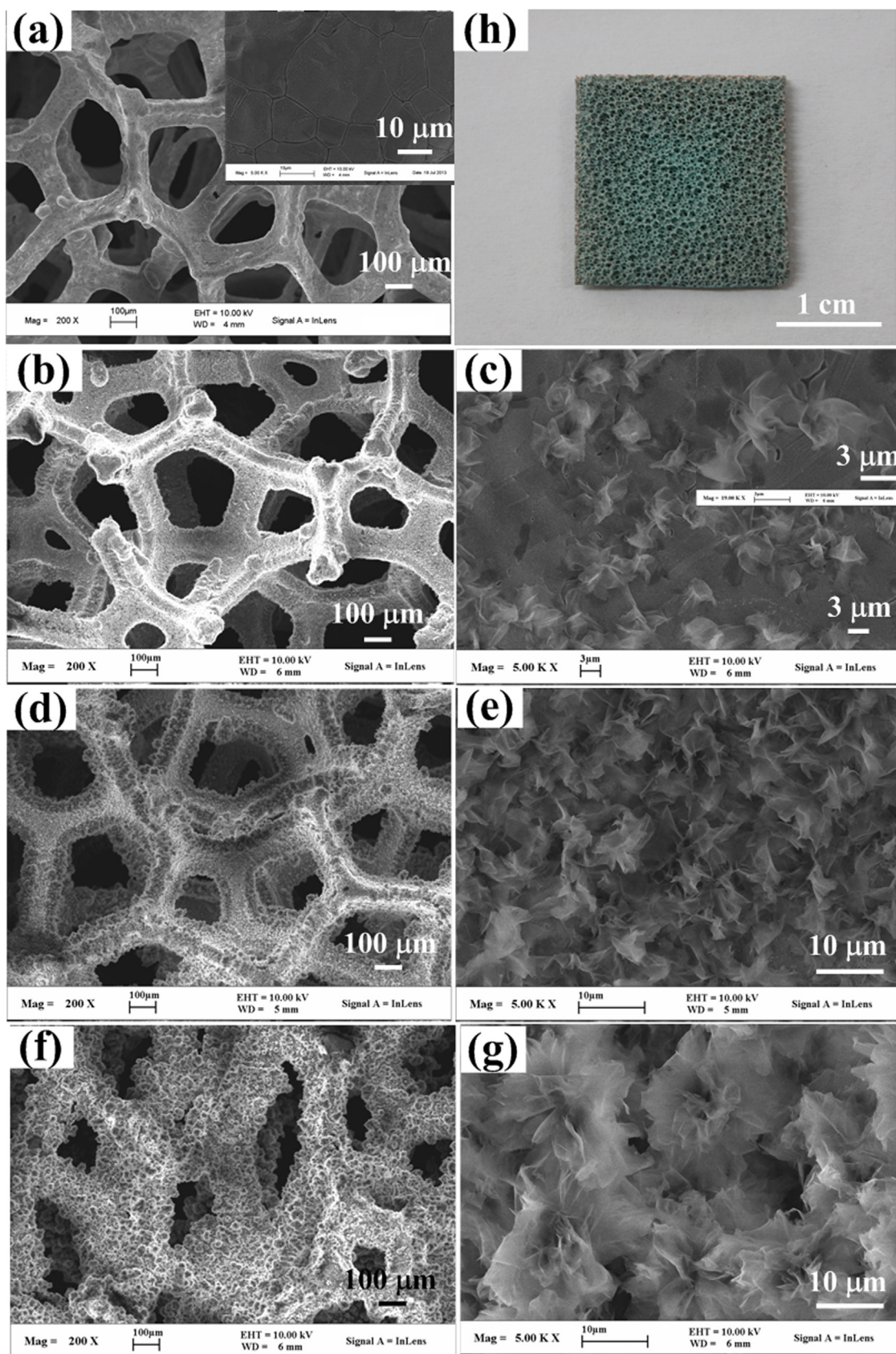


**Fig. 1.** FE-SEM images of (a) bare copper foam; and copper foams prepared via the one-step solution-immersion process with immersion times of (b) 4 h, (d) 2 days, and (f) 4 days. Images (c), (e), and (g) are higher-magnification versions of (b), (d), and (f), respectively. The insets in (a) and (c) are higher-magnification images of the bare surface and of a self-assembled cluster, respectively. (h) Photograph of the copper foam prepared with an immersion time of 4 days.



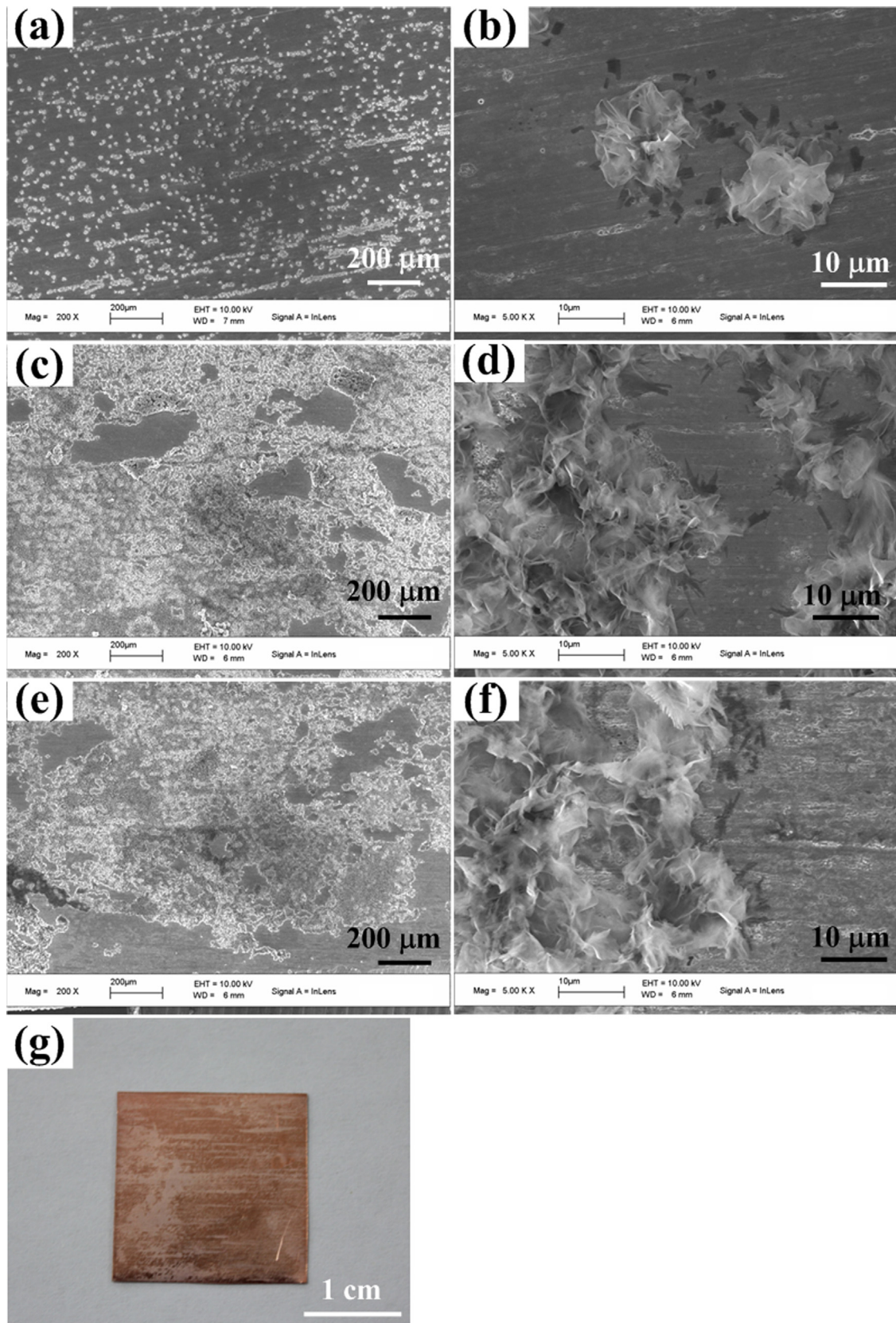


**Fig. 2.** FE-SEM images of the prepared copper plate after immersion times of (a) 4 h, (c) 2 days and (e) 4 days. Images (b), (d), and (f) are higher-magnification versions of (a), (c), and (e), respectively. (g) Photograph of the copper foam prepared using an immersion time of 4 days. (For interpretation of the references to color in this figure legend, the reader is referred to the web version of this article.)

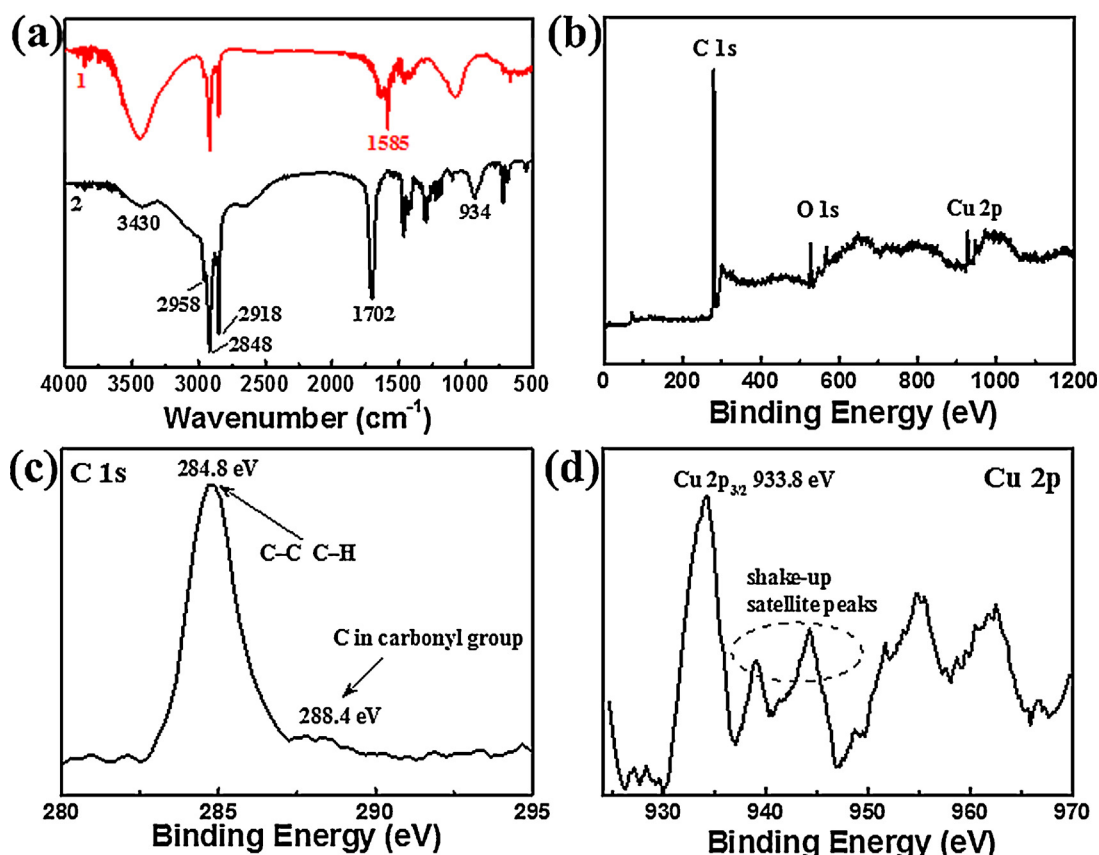


**Fig. 3.** (a) FTIR spectra of  $\text{Cu}[\text{CH}_3(\text{CH}_2)_{16}\text{COO}]_2$  (1) powder scraped from the resultant surface and stearic acid (2). (b)–(d) show the XPS spectra, C 1s and Cu 2p peaks of the resultant surface, respectively. (For interpretation of the references to color in this figure legend, the reader is referred to the web version of this article.)

A product composed of  $\text{Cu}[\text{CH}_3(\text{CH}_2)_{16}\text{COO}]_2$  was expected to be deposited on the surfaces of the copper foam and the copper plates.

As shown in the FTIR spectra (Fig. 3(a)), the two absorption bands at 2848 and 2918  $\text{cm}^{-1}$ , which are assigned to the symmetric and asymmetric stretching vibrations, respectively, of the C–H bonds in the methylene groups, and the absorption band at 2958  $\text{cm}^{-1}$  which corresponds to the asymmetric stretching vibration of the C–H bonds in the methyl group, can be observed in the spectrum of stearic acid powder as well as in the spectrum of the material scraped from the final coating deposited on the surface of the copper foams prepared with immersion times of 4 days. The peak seen at around 1702  $\text{cm}^{-1}$  in the stearic acid spectrum (and assigned to the C=O bond stretching vibration of the carboxyl group) is no longer present after the immersion process; instead, an absorption band corresponding to coordinated C=O bonds appears at 1585  $\text{cm}^{-1}$ , as expected from the formation of stearate. Some other peaks are present in the stearic acid spectrum but not in the spectrum of the deposits: the relatively broad absorption bands between 3200 and 2500  $\text{cm}^{-1}$  (corresponding to the O–H bond stretching vibration), and the peak at 934  $\text{cm}^{-1}$  (the OH...O= bond deformation vibration of the carboxyl groups). The broad peaks around 3430  $\text{cm}^{-1}$  for both powders were attributed to stretching of the O–H bonds within atmospheric adsorbed water. Thus, the films formed on the copper foams are identified as copper stearate.

XPS detected Cu, O, and C atoms (Fig. 3(b)). Fig. 3(c) and (d) shows the XPS narrow-range spectra for C 1s and Cu 2p, respectively. The main peak in the C 1s spectrum at 284.8 eV is mostly attributed to the C–C and C–H bonds [32], along with a contribution from contamination of the surface. The signal at 288.4 eV comes from the C in the carbonyl groups [32,33]. The peak at about

933.8 eV corresponds to the Cu 2p<sub>3/2</sub>, and is consistent with the reported data for Cu 2p in copper stearate [34]. The presence of the shake-up satellite peaks at the high binding-energy side of the main peak for Cu 2p<sub>3/2</sub> is characteristic of a Cu<sup>2+</sup> phase [35]. Moreover, the atomic ratio of Cu to C in the carbonyl group is calculated from the peak areas as ~1:2; this is further evidence that the material deposited on the surface of copper foam is copper(II) stearate,  $\text{Cu}[\text{CH}_3(\text{CH}_2)_{16}\text{COO}]_2$ .

Unlike the passivation of copper surfaces by the formation of a copper oxide layer in the air, copper stearate aggregates grow on the surfaces of the copper foams and plates with a cluster morphology. Such loose structure provides a continuous supplement of Cu<sup>2+</sup> ions to continue forming more flower-like clusters, as observed in the SEM. Notably, the deposition of copper stearate on the copper substrates is not based on chemical bonds. As such, external mechanical forces of gravity and buoyancy, or operations during the fabrication process, can cause flaking of the copper stearate film from the copper substrates. Some deposits were observed in the bottom of the beakers of the copper plates, and parts of the copper stearate film peeled off from the copper plates during the washing and drying processes. The tiny fiber skeleton and large specific surface area of 3D porous copper foam may allow misfit stress to relax and leave the rough copper stearate films intact.

The wettability of the prepared surfaces is characterized in detail with static water CA measurements. As shown in Fig. 4(a), the water CAs on the surface of the copper foam substrates increases with increasing immersion time. Both the bare copper plate and copper foam are noticeably hydrophilic, with the former having a water CA of 77° while the latter is superhydrophilic. A 5  $\mu\text{L}$  water droplet spreads immediately on the surface and is pulled into the porous structure by strong capillary forces. Immersion

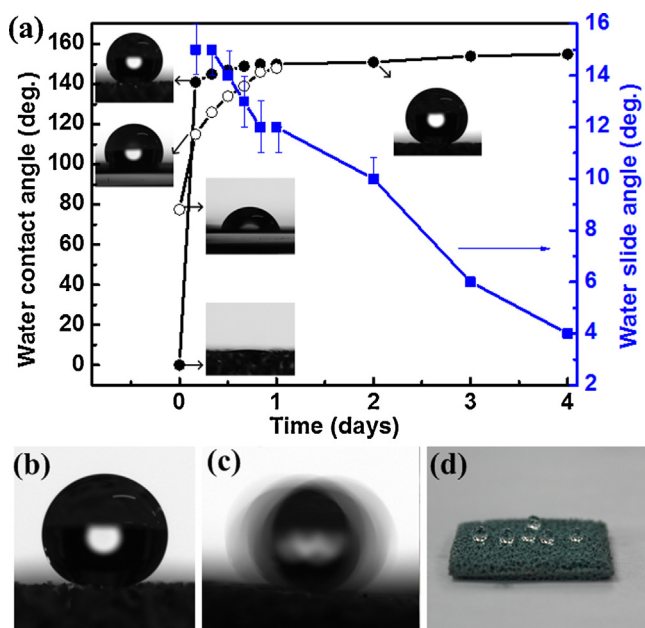


**Fig. 4.** (a) Water contact and slide angles of the prepared surfaces on the copper foams as a function of the immersion times. The water contact angles of the prepared surfaces on the copper plate are also shown for comparison (marked as hollow circles). Some photographs of water droplets on the surfaces are shown in the insets. (b) Photographs of a 5  $\mu\text{L}$  water droplet on the surface of the copper foam with an immersion time of 4 days. (c) Snapshot of the water droplet on the surface tilted at 4°. (d) Photograph of several water droplets on the prepared superhydrophobic surface on a copper foam. (For interpretation of the references to color in this figure legend, the reader is referred to the web version of this article.)

into ethanolic stearic acid solutions significantly changes the wettability. The CA of copper foam increases noticeably faster than that of the copper plate. For immersion time of only 4 h, the CA of the copper foam increases to 141° while that of copper plate is only 115°. Copper foams with immersion times longer than 2 days were found to have CAs larger than 150°. Fig. 4 (b) shows the shape of a water droplet with a CA of 156° on the prepared hydrophobic copper foam surface with an immersion time of 4 days. The CAs of the copper plates with immersion times longer than 1 day are not shown in Fig. 4 (a) as the partial flaking of copper stearate films results in a large range of CAs. For example, the CAs can be less than 90° on some exposed copper surfaces but can also be larger than 150° in areas covered by a copper stearate film.

The water SAs of copper foam depends on the immersion time are also shown in Fig. 4 (a) referring to the right-hand axis. When the immersion time exceeds 2 days, the SAs decrease to less than 10°. Fig. 4(c) shows the sliding behavior of a 5  $\mu\text{L}$  water droplet on a copper foam surface, prepared using an immersion time of 4 days. When the surface is tilted by 4°, the water droplet immediately rolls off. This indicates that superhydrophobic surfaces can be fabricated on copper foams using the one-step immersion approach; a photograph of droplets on such a surface is shown in Fig. 4(d). It is notable that the self-assembled second layer of flowerlike copper stearate clusters, as shown in the SEM images (Fig. 1(g)), is crucial to the reduction of the SAs. Even though the CA of the prepared copper foam with an immersion time of 2 days is larger than 150°, the water droplet cannot easily roll off as there is a strong resistance from the large surface pores that have not been significantly decreased in size by the deposition of copper stearate clusters. With the further deposition of copper stearate, the flowerlike clusters are formed, and the dimensions of the surface pores are greatly reduced, providing for the opportunity for water droplets to easily roll off. The highest CA for the superhydrophobic copper stearate films obtained here on copper foam (156°) lies between the previously reported

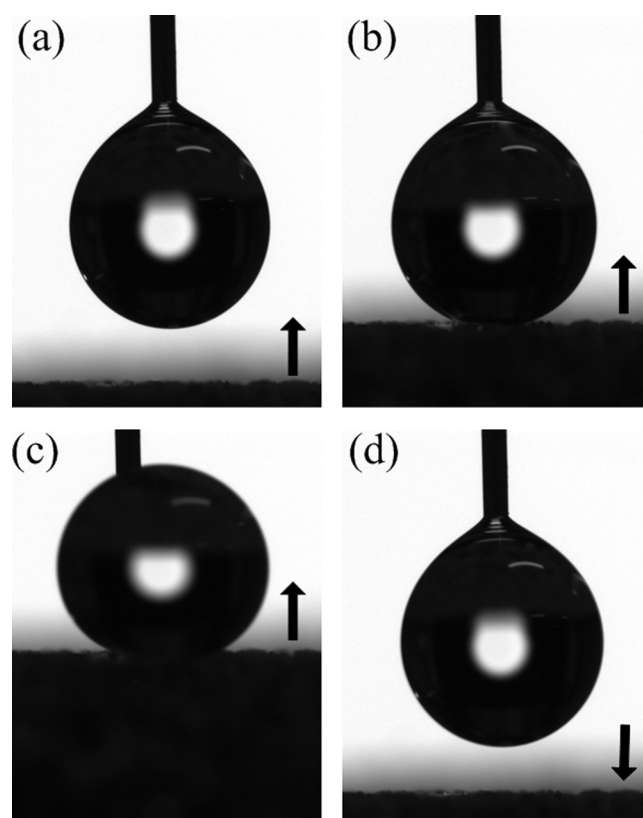


**Fig. 5.** Sequential photographs of a 4  $\mu\text{L}$  water droplet (a) suspended on a syringe, (b) just touching, (c) excessively contacted with the lifting substrate, and (d) leaving the lowering surface. The arrows show the direction of movement of the substrate.

CAs for superhydrophobic copper stearate films on flat copper substrates fabricated by spraying (160°) [25] or by electrodeposition (153°) [24]. However, the SA here is slightly larger than those of the two previously reported superhydrophobic films, (3° for [25] and 1.3° for [24]). This can be attributed to the unevenness of our original copper foam substrates.

Fig. 5 shows the non-sticking behavior of superhydrophobic copper foam surfaces. A 4  $\mu\text{L}$  water droplet is first suspended on a needle (Fig. 5(a)). The copper foam surface is then lifted to come into contact with the water droplet (Fig. 5(b)). However, the suspending droplet cannot be pulled down to the copper foam surface. Even if the copper foam surface is raised so that the needle is inserted into the droplet (Fig. 5(c)), the water droplet is still hanging on the needle after it departs from the copper foam surfaces (Fig. 5(d)). After this process, the copper foam surface repeatedly comes into contact with the water droplet and departs. This occurs several times with the droplet still intact.

Abrasion tests were carried out to evaluate the mechanical robustness of the superhydrophobic surfaces prepared on the copper foam and copper plate substrates with immersion times of 4 days. Details of this test have been described in Part 2. After the abrasion test, almost all the surface covering on the copper plate had been worn off (Fig. 6(a)). However, there was no change to the outward appearance of the superhydrophobic surfaces on the copper foam substrate (inset in Fig. 6(b)). The SEM image of the copper stearate coverings on the copper foam substrates (Fig. 6(b)) show that some coverings on the tips of the 3D porous skeleton have been worn off. Abrasion of our superhydrophobic surfaces on copper foams decreases their CAs and increases their SAs to mean values of 151° and  $\sim$ 10°, respectively. Although some degradation takes place, we have confirmed that the superhydrophobic surfaces on copper foams are more robust



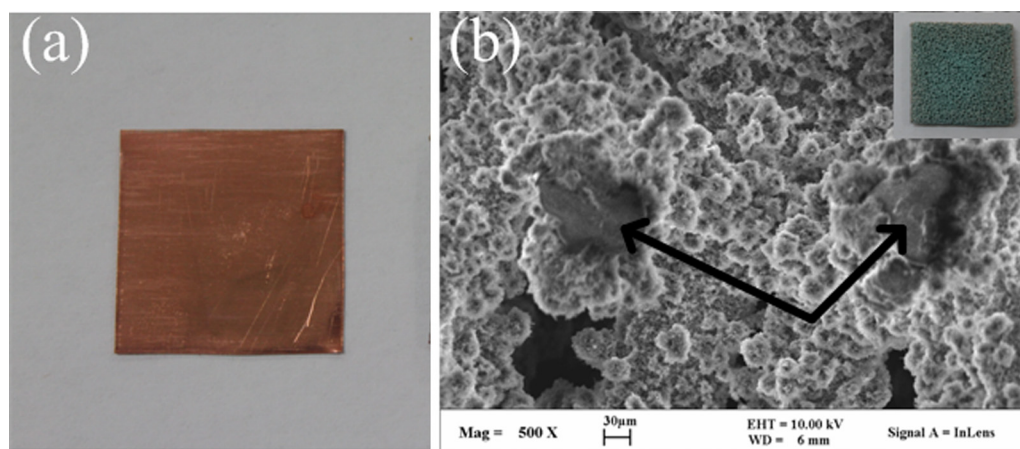


**Fig. 6.** (Color online) (a) Photograph of a prepared copper plate with an immersion time of 4 days after the abrasion test. (b) SEM image of the superhydrophobic copper foam after the abrasion test. The arrows point out the areas bare of Cu where the layers of copper stearate have been worn off. Its photograph is shown in the upper right inset.

than those on copper plates. Decreases in CAs after abrasion tests have been previously reported: for example, from  $170^\circ$  to  $153^\circ$ , and from  $169^\circ$  to  $144^\circ$ , respectively, for superhydrophobic surfaces on copper [20] and aluminum [31]. In our case, the retention of  $CA > 150^\circ$  for the superhydrophobic surfaces on copper foams after abrasion is mainly attributed to the natural unevenness of the copper foams, which meant that some protrusions bore most of the pressure during the abrasion tests. A similar mechanism was also found for abrasion-resistance of superhydrophobic surfaces on selectively-etched  $\{110\}$  facets of copper foils [20]. In contrast, when superhydrophobic surfaces on flat substrates (such as on aluminum foil [31] and on the copper plates in our experiment) are subjected to abrasion testing, the entire surface experiences contact and thus friction, leading to more significant decreases in superhydrophobicity.

#### 4. Conclusions

Non-flaking superhydrophobic surfaces have been fabricated on copper foam substrates by a one-step solution-immersion process. The cleaned copper foams are immersed in ethanolic stearic acid solution at room temperature for about 4 days and form hierarchical micro-/nano-structures on the surfaces. The resultant surface exhibits superhydrophobicity with a water CA of  $156^\circ$  and a SA of  $4^\circ$ . Non-sticking behavior has been demonstrated. Compared with flat copper plates, the superhydrophobic surface on copper foam are much more robust with better mechanical stability. The technique employed here, where commercially obtained 3D porous structures are used as substrates for the one-step solution-immersion process, is a facile approach to fabricate stable superhydrophobic surfaces. This is readily scalable for the fabrication of large superhydrophobic surface areas. The present study may lead to the further development of practical applications for superhydrophobic copper foams.

#### Acknowledgement

The authors thank the National Science Foundation of China (Grant Nos. 11004054, U1034004, 51211130118, 11104283, 51210011), the Fundamental Research Funds for the Central Universities, the Open Research Fund Program of the State Key Laboratory of Low-Dimensional Quantum Physics (Grant No. KF201207) and the Royal Society–China NSFC joint project (2012–2014).

#### References

- [1] Y.Y. Yan, N. Gao, W. Barthlott, Mimicking natural superhydrophobic surfaces and grasping the wetting process: a review on recent progress in preparing superhydrophobic surfaces, *Adv. Colloid Interface Sci.* 169 (2011) 80–105.
- [2] X. Yao, Y.L. Song, L. Jiang, Applications of bio-inspired special wettable surfaces, *Adv. Mater.* 23 (2011) 719–734.
- [3] K.S. Liu, L. Jiang, Metallic surfaces with special wettability, *Nanoscale* 3 (2011) 825–838.
- [4] N. Verplanck, Y. Coffinier, V. Thomy, R. Boukherroub, Wettability switching techniques on superhydrophobic surfaces, *Nanoscale Res. Lett.* 2 (2007) 577–596.
- [5] L. Feng, Z.Y. Zhang, Z.H. Mai, Y.M. Ma, B.Q. Liu, L. Jiang, D.B. Zhu, A superhydrophobic and super-oleophilic coating mesh film for the separation of oil and water, *Angew. Chem. Int. Ed.* 43 (2004) 2012–2014.
- [6] C.F. Carlborg, W. van der Wijngaart, Sustained superhydrophobic friction reduction at high liquid pressures and large flows, *Langmuir* 27 (2011) 487–493.
- [7] H.Q. Liu, S. Szunerits, W.G. Xu, R. Boukherroub, Preparation of superhydrophobic coatings on zinc as effective corrosion barriers, *ACS Appl. Mater. Interfaces* 1 (2009) 1150–1153.
- [8] D. Byun, J. Kim, H.S. Ko, H.C. Park, Direct measurement of slip flows in superhydrophobic microchannels with transverse grooves, *Phys. Fluids* 20 (2008) 113601.
- [9] M. Joansson-Niedziolka, F. Lapiere, Y. Coffinier, S.J. Parry, F. Zoueshtigh, T. Foat, V. Thomy, R. Boukherroub, EWOD driven cleaning of bioparticles on hydrophobic and superhydrophobic surfaces, *Lab Chip* 11 (2011) 490–496.
- [10] F. Lapiere, G. Piret, H. Drobecq, O. Melnyk, Y. Coffinier, V. Thomy, R. Boukherroub, High sensitive matrix-free mass spectrometry analysis of peptides using silicon nanowires-based digital microfluidic device, *Lab Chip* 11 (2011) 1620–1628.
- [11] J.B. Boreyko, C.H. Chen, Self-propelled dropwise condensate on superhydrophobic surfaces, *Phys. Rev. Lett.* 103 (2009) 184501.
- [12] Y. Huang, D.K. Sarkar, D. Gallant, X.G. Chen, Corrosion resistance properties of superhydrophobic copper surfaces fabricated by one-step electrochemical modification process, *Appl. Surf. Sci.* 282 (2013) 689–694.
- [13] Z.Z. Zhang, X.T. Zhu, J. Yang, X.H. Xu, X.H. Men, X.Y. Zhou, Facile fabrication of superoleophobic surfaces with enhanced corrosion resistance and easy reparability, *Appl. Phys. A* 108 (2012) 601–606.
- [14] S.J. Yuan, S.O. Pehkonen, B. Liang, Y.P. Ting, K.G. Neoh, E.T. Kang, Superhydrophobic fluoropolymer-modified copper surface via surface graft polymerisation for corrosion protection, *Corros. Sci.* 53 (2011) 2738–2747.
- [15] I.A. Larmour, S.E.J. Bell, G.C. Saunders, Remarkably simple fabrication of superhydrophobic surfaces using electroless galvanic deposition, *Angew. Chem. Int. Ed.* 46 (2007) 1710–1712.
- [16] Y.H. Fan, C.Z. Li, Z.J. Chen, H. Chen, Study on fabrication of the superhydrophobic sol-gel films based on copper wafer and its anti-corrosive properties, *Appl. Surf. Sci.* 258 (2012) 6531–6536.
- [17] Z.G. Guo, W.M. Liu, B.L. Su, A stable lotus-leaf-like water-repellent copper, *Appl. Phys. Lett.* 92 (2008) 063104.
- [18] X. Yao, L.A. Xu, L. Jiang, Fabrication and characterization of superhydrophobic surfaces with dynamic stability, *Adv. Funct. Mater.* 20 (2010) 3343–3349.
- [19] W.J. Xi, Z.M. Qiao, C.L. Zhu, A. Jia, M. Li, The preparation of lotus-like superhydrophobic copper surfaces by electroplating, *Appl. Surf. Sci.* 255 (2009) 4836–4839.
- [20] L.J. Liu, F.Y. Xu, L. Ma, Facile fabrication of a superhydrophobic Cu surface via a selective etching of high-energy facets, *J. Phys. Chem. C* 116 (2012) 18722–18727.

- [21] H.Q. Liu, S. Szunerits, M. Pisarek, W.G. Xu, R. Boukherroub, Preparation of superhydrophobic coatings on zinc, silicon, and steel by a solution-immersion technique, *ACS Appl. Mater. Interfaces* 9 (2009) 2086–2091.
- [22] S.T. Wang, L. Feng, L. Jiang, One-step solution-immersion process for the fabrication of stable bionic superhydrophobic surfaces, *Adv. Mater.* 18 (2006) 767–770.
- [23] J.M. Xi, L. Feng, L. Jiang, A general approach for fabrication of superhydrophobic and superamphiphobic surfaces, *Appl. Phys. Lett.* 92 (2008) 053102.
- [24] Y. Huang, D.K. Sarkar, X.G. Chen, A one-step process to engineer superhydrophobic copper surfaces, *Mater. Lett.* 64 (2010) 2722–2724.
- [25] J. Li, H.Q. Wan, Y.P. Ye, H.D. Zhou, J.M. Chen, One-step process for the fabrication of superhydrophobic surfaces with easy repairability, *Appl. Surf. Sci.* 258 (2012) 3115–3118.
- [26] K.L. Zhang, C. Rossi, C. Tenailleau, P. Alphonse, J.Y. Chane-Ching, Synthesis of large-area and aligned copper oxide nanowires from copper thin film on silicon substrate, *Nanotechnology* 18 (2007) 275607.
- [27] Y. Li, W.Z. Jia, Y.Y. Song, X.H. Xia, Superhydrophobicity of 3D porous copper films prepared using the hydrogen bubble dynamic template, *Chem. Mater.* 19 (2007) 5758–5764.
- [28] Y.P. Yang, X.B. Ji, J.L. Xu, Pool boiling heat transfer on copper foam covers with water as working fluid, *Int. J. Therm. Sci.* 49 (2010) 1227–1237.
- [29] M.R.S. Shirazy, S. Blais, L.G. Fréchette, Mechanism of wettability transition in copper metal foams: from superhydrophilic to hydrophobic, *Appl. Surf. Sci.* 258 (2012) 6416–6424.
- [30] Y.H. Xiu, Y. Liu, D.W. Hess, C.P. Wong, Mechanically robust superhydrophobicity on hierarchically structured Si surfaces, *Nanotechnology* 21 (2010) 155705.
- [31] L.J. Liu, J.S. Zhao, Y. Zhang, F. Zhao, Y.B. Zhang, Fabrication of superhydrophobic surface by hierarchical growth of lotus-leaf-like boehmite on aluminum foil, *J. Colloid Interface Sci.* 358 (2011) 277–283.
- [32] N.N. Yao, P. Zhang, L.X. Song, M. Kang, Z.Y. Lu, R. Zheng, Stearic acid coating on circulating fluidized bed combustion fly ashes and its effect on the mechanical performance of polymer composites, *Appl. Surf. Sci.* 279 (2013) 109–115.
- [33] L. Zhang, L. Chen, H.Q. Wan, J.M. Chen, H.D. Zhou, Synthesis and tribological properties of stearic acid-modified anatase (TiO<sub>2</sub>) nanoparticles, *Tribol. Lett.* 41 (2011) 409–416.
- [34] S. Li, H.Z. Wang, W.W. Xu, H.L. Si, X.J. Tao, S.Y. Lou, Z.L. Du, L.S. Li, Synthesis and assembly of monodisperse spherical Cu<sub>2</sub>S nanocrystals, *J. Colloid Interface Sci.* 330 (2009) 483–487.
- [35] J. Xu, J.L. Sun, J.Q. Wei, J.L. Xu, The wavelength dependent photovoltaic effects caused by two different mechanisms in carbon nanotube film/CuO nanowire array heterodimensional contacts, *Appl. Phys. Lett.* 100 (2012) 251113.